Current Biology

Natural variation in ELF3 controls thermoresponsive growth in Arabidopsis

--Manuscript Draft--

Manuscript Number:	CURRENT-BIOLOGY-D-14-00888R1
Full Title:	Natural variation in ELF3 controls thermoresponsive growth in Arabidopsis
Article Type:	Report
Corresponding Author:	Philip Anthony Wigge, Ph.D Cambridge University Cambridge, UNITED KINGDOM
First Author:	Philip Anthony Wigge, Ph.D
Order of Authors:	Philip Anthony Wigge, Ph.D
	Mathew S Box
	B Emma Huang
	Mirela Domijan
	Katja E Jaeger
	Asif Khan Khattak
	Seong Jeon Yoo
	Emma L Sedivy
	D Marc Jones
	Timothy J Hearn
	Alex A.R. Webb
	Alastair Grant
	James C. W. Locke
Abstract:	Plant development is highly responsive to ambient temperature, and this trait has been linked to the ability of plants to adapt to climate change. The mechanisms by which natural populations modulate their thermoresponsiveness are not known. To address this, we surveyed Arabidopsis accessions for variation in thermal responsiveness of elongation growth and mapped the corresponding loci. We find that the transcriptional regulator EARLY FLOWERING3 (ELF3) controls elongation growth in response to temperature. Through a combination of modeling and experiments, we show that high temperature relieves the gating of growth at night, highlighting the importance of temperature dependent repressors of growth. ELF3 gating of transcriptional targets responds rapidly and reversibly to changes in temperature. We show that the binding of ELF3 to target promoters is temperature dependent, suggesting a mechanism where temperature directly controls ELF3 activity.

Title: Natural variation in *ELF3* controls thermoresponsive growth in Arabidopsis

Authors:

Mathew S. Box[1], B. Emma Huang[2], Mirela Domijan[1], Katja E. Jaeger[1], Asif Khan Khattak[3,4], Seong Jeon Yoo[1], Emma L. Sedivy[1†], D. Marc Jones[1‡], Timothy J. Hearn[5], Alex A. R. Webb[5], Alastair Grant[4], James C. W. Locke[1], Philip A. Wigge[1*]

Affiliations:

[1] The Sainsbury Laboratory, University of Cambridge, Cambridge, CB2 1LR, UK.

[2] CSIRO, Dutton Park, Queensland, Australia.

[3] John Innes Centre, Norwich Research Park, Norwich, NR4 7UH, UK.

[4] University of East Anglia, School of Environmental Sciences, Norwich, UK.

[5] Department of Plant Sciences, University of Cambridge, Cambridge, CB2 3EA, UK.

[†] Current address: Department of Biology, Massachusetts Institute of Technology, Cambridge, MA, USA.

[‡] Current address: John Innes Centre, Norwich Research Park, Norwich, NR4 7UH, UK.

* Correspondence to: philip.wigge@slcu.cam.ac.uk

Summary:

Plant development is highly responsive to ambient temperature, and this trait has been linked to the ability of plants to adapt to climate change [1]. The mechanisms by which natural populations modulate their thermoresponsiveness are not known [2]. To address this, we surveyed Arabidopsis accessions for variation in thermal responsiveness of elongation growth and mapped the corresponding loci. We find that the transcriptional regulator *EARLY FLOWERING3* (*ELF3*) controls elongation growth in response to temperature. Through a combination of modeling and experiments, we show that high temperature relieves the gating of growth at night, highlighting the importance of temperature dependent repressors of growth. ELF3 gating of transcriptional targets responds rapidly and reversibly to changes in temperature. We show that the binding of ELF3 to target promoters is temperature dependent, suggesting a mechanism where temperature directly controls ELF3 activity.

One Sentence Summary:

Natural variation in ELF3 modulates thermoresponsive elongation growth in *Arabidopsis thaliana*.

Results and Discussion:

Plants are sensitive to small differences in temperature, and the phenology and distribution of wild plants has already been altered by climate change [1]. The ability of species to survive climate change is linked to their capacity to adjust their development in response to temperature, resulting in phylogenetic patterns of species loss [2]. To understand how warm temperature influences the day-night growth cycle, we analysed thermoresponsive elongation growth in Arabidopsis. At 27 ºC, plants have increased levels of the phytohormone auxin, which triggers hypocotyl elongation [3] (Figure 1A). This is controlled by the bHLH transcription factor PHYTOCHROME INTERACTING FACTOR4 (PIF4) [3–5]. As expected, elongation growth at 22 ºC is gated (Figure 1B), occurring just before dawn [6, 7]. At 27 ºC the maximal growth rate is about twice that of 22 ºC, and growth occurs throughout the first night following germination, with peaks at dusk and dawn in subsequent nights [8] (Figure 1B). Light mediated growth repression is maintained at 27 ºC, indicating that the thermoresponsive growth pathway acts by relieving night-time growth repression.

To identify natural variation in this trait, we analysed thermoresponsive elongation growth for 19 Arabidopsis natural accessions from a wide geographic range (the MAGIC parental lines [9]). Within these accessions, warmer temperatures cause large differences in hypocotyl length, indicating significant genetic variation in this trait (Figure 1C). Columbia-0 is one of the less responsive genotypes in this collection, showing robust growth repression at 22 ºC. To understand this genetic variation in more detail, we surveyed thermoresponsive growth within the MAGIC RIL population, which have been derived by intercrossing the 19 MAGIC parents [9]. This revealed highly heritable transgressive segregation, indicating the interaction of multiple genes in these backgrounds contribute to this trait (Figure 1D and Table S1).

Hypocotyl length data at different temperatures (Figure 1D) as well as thermal responsiveness values obtained from pairwise subtractive comparisons and fitting a multivariate model, were used to map QTL. This enabled us to identify genetic interactions for hypocotyl length at each individual temperature as well as determine if

there are QTL responsible for variation in responsiveness to temperature. In total, seven QTL were detected across the three temperatures (Figure 1E, Figure S1 and Table S2)

Three major QTL accounting for a significant proportion of the observed phenotypic variation (Figure 1E and Table S2) were mapped to intervals containing an over-representation of genes involved in gating hypocotyl elongation in response to environmental and endogenous cues (*PHYB*, *PHYE*, *ELF3* and *LUX*). Strikingly, the QTL on chromosome 2 (HL22.2), containing *ELF3* as a candidate, is temperature dependent, disappearing at 27 ºC, suggesting that the locus is involved in a gene by environment interaction.

We estimated founder allele effects via multiple imputation in R/happy [9] for the QTL for hypocotyl length variation at 22 ºC on chromosomes 2 and 3. This allowed us to quantitatively estimate the contribution of alleles from each MAGIC parent to the observed QTL (Figure 2A and Figure S2). By this method we identified MAGIC parents Ct-1, No-0, Sf-2, Tsu-0 and Zu-0 as significant contributors to the QTL containing the candidate genes *PHYB*, *ELF3* and *LUX* and quantitatively estimated the relative strength of each allele with respect to hypocotyl length in each parental line.

Since *ELF3* and *LUX* encode components of the Evening Complex (EC), which gates hypocotyl elongation [10–13], we sought to determine if they were the genes underlying the QTL. The EC is required for circadian clock function in continuous light [14, 15], and therefore we tested a selection of the MAGIC parental lines for circadian function. Consistent with these accessions having altered EC function, some of the major parental lines contributing to the *ELF3* and *LUX* QTL have less robust circadian rhythms as indicated by their relative amplitude error (RAE; Figure 2B and Figure S2). For example Sf-2, which is a major contributing parent to the chromosome 2 QTL at 22 ºC (HL22.2), has one of the least rhythmic clocks in this assay and is predicted to carry a weak allele of *ELF3* in our allele effect estimates (Figure 2A).

To confirm that these candidate genes are responsible for altered

thermoresponsiveness, we tested the allele effect estimates directly by selecting a representative range of parental lines predicted to have different strengths of *PHYB*, *ELF3* and *LUX* alleles and carried out quantitative complementation crosses to the null alleles *phyb-9, elf3-1* and *lux-4*. While the long hypocotyl phenotypes of these parental lines are rescued in the F1 of the Col-0 crosses, *phyb-9*, *elf3-1* and *lux-4* mutants show quantitative rescue that corresponds with the predicted allele effect estimates in the range of parental lines tested (Figures 2A and 2C). Moreover they are unable to rescue the long hypocotyl response in the F1 of Sf-2 and Ct-1, showing that these genes contribute significantly to the phenotypes we observe (Figure 2C) and are the quantitative trait genes underlying the Chromosome 2 and Chromosome 3 QTL at 22 ºC. This is consistent with a recent study which also linked *ELF3* and *LUX* activity to thermoresponsive growth [16].

As the accessions Sf-2, Tsu-0 and Ct-1 show greater thermoresponsive growth and have been shown to carry weak alleles for *ELF3* and *LUX*, we examined their growth dynamics at 22 ºC. Consistent with their warm temperature phenotype, all these backgrounds show significantly higher night-time growth rates compared to Col-0 (Figure 2D and Figure S2). As these backgrounds are predicted to retain some *ELF3* and *LUX* activity, we tested the thermoresponsive growth of *elf3-1* and *lux-4*. At 22 ºC, both these backgrounds show enhanced growth early in the evening, while daytime growth repression is maintained (Figures 2E, 2F and Figure S2). While *lux-4* growth retains thermoresponsiveness, the growth dynamics of *elf3-1* at 22 ºC are similar to Col-0 at 27 ºC. Indeed, *elf3-1* shows very little difference in its growth dynamics between 22 ºC and 27 ºC, suggesting it has a constitutive warm temperature response at 22 ºC (Figure 2E).

As warm temperature signals relieve growth repression, and this is modulated by natural variation in *ELF3* and *LUX*, we sought to determine where in the pathway temperature information is integrated. To assay the activity of the temperature dependent growth repression pathway we examined the expression of *PIF4*, since this gene is necessary and sufficient for thermoresponsiveness [4, 17]. In Col-0 there is a characteristic gating of *PIF4* expression at 22 ºC, with a peak of expression occurring

just before dawn [18]. At 27 ºC, this peak of *PIF4* expression is increased about two-fold (Figure 3A). A key transcriptional target of PIF4 is *ARABIDOPSIS THALIANA HOMEOBOX PROTEIN-2 (ATHB-2)*, which encodes a transcription factor controlling growth regulation [19]. Using *ATHB-2* expression as a proxy for PIF4 functional activity, we find that the peak of *ATHB-2* expression coincides with that of *PIF4* (Figure 3B). Since the accessions Ct-1, Sf-2 and Tsu-0 have enhanced night-time growth (Figure 2D), we predicted them to show greater *PIF4* and *ATHB-2* expression at night, which is the case (Figures 3A and 3B). Since it has been shown in other backgrounds that mutations in *ELF3* affecting nuclear localisation perturb function [20], we examined the *ELF3* coding region in Sf-2, which we have shown to be a weak allele. While no changes in the *ELF3* protein-coding region could be found in Sf-2 compared to Col-0 (Figure S3), the expression of *ELF3* in Sf-2 is significantly lower than Col-0. This expression difference likely accounts for the decreased *ELF3* activity in Sf-2 (Figure 3C). To determine if the thermosensory response might be a consequence of temperature-dependent expression of *ELF3* and *LUX*, we analysed the expression of these genes at 22 and 27 ºC. *ELF3* and *ELF4* show no temperature responsiveness in their expression, while *LUX* expression actually increases at higher temperatures (Figures 3C-E and Figure S4). The effect of warm temperature on growth is therefore not mediated through transcriptional regulation of the genes of the EC.

To understand the control of thermoresponsive growth, we modelled the expression of *PIF4* with gating by a general repressor, R. A light dependent repressor, P, mediates the rapid morning shutdown of *PIF4* expression. This is captured in the equation for *PIF4* production rate (Supplementary Experimental Procedures). We used our expression data for *PIF4* in Col-0 to parameterize this model. This revealed that decreasing R activity at higher temperature is sufficient to account for the dynamics of expression we observe in Col-0 (Figure 4A). Since it has been proposed that warm temperature signals are mediated by the Evening Complex (EC) [16], we simulated this scenario in our model by assigning all the activity of R to the EC. If the EC is solely responsible for the activity of R, setting R = 0 should capture the dynamics of *PIF4* expression in *elf3-1* and *lux-4*, as these backgrounds lack a functional EC. While this

model largely recapitulates the end of night expression observed for *PIF4* in *lux-4* and *elf3-1*, it has a poor fit with the expression of *PIF4* at the beginning and in the middle of the night in these backgrounds (Figure 4A). This suggests that temperature-dependent EC activity is not sufficient to account for the growth responses we observe. We therefore re-ran our simulations to capture *PIF4* expression in *lux-4* and *elf3-1*, by modulating R whilst keeping all other parameters fixed to the Col-0 values (Supplementary Experimental Procedures). Doing so was sufficient for the models to capture the behavior of *PIF4* in *lux-4* and *elf3-1* (Figure 4A). While EC activity is required to maintain repression of *PIF4* at both 22 and 27 ºC, activity of the EC itself does not appear to be responsive to temperature, since *PIF4* expression in *lux-4*, while higher, is still thermoresponsive. To quantify this, we extracted the level of repressor activity from the area under the curves for R expression, and scaled this by the median level of expression at 27 ºC in each background (Figure 4B and Figure S4). This shows that the difference in R activity in the *lux-4* background between 22 and 27 ºC is similar to that observed in Col-0, which is not the case for *elf3-1*. Our modeling and expression data therefore indicate that while *lux-4* retains a degree of thermoresponsiveness comparable to wildtype, *elf3*-1 does not. We therefore conclude that *ELF3* is a key node required for transmitting temperature information to gate evening growth. This analysis is consistent with studies showing that *elf3* mutants are unable to integrate temperature information into the clock [21] and *ELF3* acts through EC-dependent and independent pathways [11, 22].

This model indicates that *ELF3* is the key mediator of temperature signalling. Since *ELF3* is part of the circadian clock, this role could be indirect. To test how rapidly this system responds to warm temperature, we performed experiments at the end of a short day shifting seedlings between 22 and 27 ºC. To measure ELF3 activity, we assayed *LUX* expression, since this gene is directly transcriptionally repressed by ELF3 (Figures 3D and 4C). As seen before, plants grown at a constant 22 ºC show a sharp down-regulation of *LUX* expression in the evening (Figure 4C). Conversely, at 27 ºC, *LUX* expression remains higher, reflecting reduced *ELF3* activity. Plants shifted from 22 ºC to 27 ºC show a rapid upregulation of *LUX* that occurs within 2 hours. This temperature

modulated activity of *ELF3* is both rapid and reversible, since within 1 hour of being transferred from 27 ºC to 22 ºC, shifted plants exhibit as much repression of *LUX* as those grown at constant 22 ºC. This transcriptional thermoresponsiveness is controlled by *ELF3*, since temperature has no influence on *LUX* expression in *elf3-1* (Figure 4C). Taken together, our modelling and experimental results indicate that while the Evening Complex is required for the general gating of evening growth, temperature signaling is mediated by *ELF3*. The rapid responsiveness of *LUX* expression to temperature change lead us to hypothesize that temperature might directly influence ELF3 activity. ELF3 functions in the nucleus as a transcriptional repressor, and has been shown to bind target gene promoters [10, 14, 16, 23, 24]. Consistent with this, plants shifted from 22 ºC to 27 ºC for just two hours, exhibit a significant decrease in ELF3 binding to the promoters of *PRR9*, *LUX* and *PIF4* (Figure 4D). ELF4 has been shown to bind ELF3 [10, 13], and shows a similar trend with reduced binding at 27 ºC for the same promoter sites. The rapid change in the affinity of ELF3 for its targets, within 2 hours of a temperature shift, is consistent with a model where temperature directly alters ELF3 activity. *PIF4* and *ELF3* are emerging as key hubs for integrating developmental responses to the environment [4, 17, 20, 25, 26], and it will be interesting to see if their role in thermoresponsiveness is conserved in crop plants.

References:

1. Fitter, A. H., and Fitter, R. S. (2002). Rapid changes in flowering time in British plants. Science (80-.). *296*, 1689–1691. Available at: http://www.ncbi.nlm.nih.gov/entrez/query.fcgi?cmd=Retrieve&db=PubMed&dopt=Citation&list_uids=12040195.

2. Willis, C. G., Ruhfel, B., Primack, R. B., Miller-Rushing, A. J., and Davis, C. C. (2008). Phylogenetic patterns of species loss in Thoreau's woods are driven by climate change. Proc Natl Acad Sci U S A *105*, 17029–17033. Available at: http://www.ncbi.nlm.nih.gov/entrez/query.fcgi?cmd=Retrieve&db=PubMed&dopt=Citation&list_uids=18955707.

3. Gray, W. M., Ostin, A., Sandberg, G., Romano, C. P., and Estelle, M. (1998). High temperature promotes auxin-mediated hypocotyl elongation in Arabidopsis. Proc Natl Acad Sci U S A *95*, 7197–7202. Available at: http://www.ncbi.nlm.nih.gov/entrez/query.fcgi?cmd=Retrieve&db=PubMed&dopt=Citation&list_uids=9618562.

4. Koini, M. A., Alvey, L., Allen, T., Tilley, C. A., Harberd, N. P., Whitelam, G. C., and Franklin, K. A. (2009). High temperature-mediated adaptations in plant architecture require the bHLH transcription factor PIF4. Curr Biol *19*, 408–413. Available at: http://www.ncbi.nlm.nih.gov/entrez/query.fcgi?cmd=Retrieve&db=PubMed&dopt=Citation&list_uids=19249207.

5. Franklin, K. A., Lee, S. H., Patel, D., Kumar, S. V, Spartz, A. K., Gu, C., Ye, S., Yu, P., Breen, G., Cohen, J. D., et al. (2011). Phytochrome-interacting factor 4 (PIF4) regulates auxin biosynthesis at high temperature. Proc. Natl. Acad. Sci. U. S. A. *108*, 20231–20235. Available at: http://www.ncbi.nlm.nih.gov/pubmed/22123947.

6. Nozue, K., Covington, M. F., Duek, P. D., Lorrain, S., Fankhauser, C., Harmer, S. L., and Maloof, J. N. (2007). Rhythmic growth explained by coincidence between internal and external cues. Nature *448*, 358–361. Available at: http://www.ncbi.nlm.nih.gov/entrez/query.fcgi?cmd=Retrieve&db=PubMed&dopt=Citation&list_uids=17589502.

7. Stewart, J. L., Maloof, J. N., and Nemhauser, J. L. (2011). PIF genes mediate the effect of sucrose on seedling growth dynamics. PLoS One *6*.

8. Nemhauser, J. L., Mockler, T. C., and Chory, J. (2004). Interdependency of brassinosteroid and auxin signaling in Arabidopsis. PLoS Biol *2*, E258. Available at:

http://www.ncbi.nlm.nih.gov/entrez/query.fcgi?cmd=Retrieve&db=PubMed&dopt=Citation&list_uids=15328536.

9. Kover, P. X., Valdar, W., Trakalo, J., Scarcelli, N., Ehrenreich, I. M., Purugganan, M. D., Durrant, C., and Mott, R. (2009). A multiparent advanced generation inter-cross to fine-map quantitative traits in Arabidopsis thaliana. PLoS Genet. *5*.

10. Nusinow, D. A., Helfer, A., Hamilton, E. E., King, J. J., Imaizumi, T., Schultz, T. F., Farré, E. M., and Kay, S. A. (2011). The ELF4-ELF3-LUX complex links the circadian clock to diurnal control of hypocotyl growth. Nature *475*, 398–402.

11. Kolmos, E., Herrero, E., Bujdoso, N., Millar, A. J., Toth, R., Gyula, P., Nagy, F., and Davis, S. J. (2011). A Reduced-Function Allele Reveals That EARLY FLOWERING3 Repressive Action on the Circadian Clock Is Modulated by Phytochrome Signals in Arabidopsis. Plant Cell *23*, 3230–3246. Available at: <Go to ISI>://000296739100016.

12. Jiménez-Gómez, J. M., Wallace, A. D., and Maloof, J. N. (2010). Network analysis identifies ELF3 as a QTL for the shade avoidance response in arabidopsis. PLoS Genet. *6*.

13. Herrero, E., Kolmos, E., Bujdoso, N., Yuan, Y., Wang, M., Berns, M. C., Uhlworm, H., Coupland, G., Saini, R., Jaskolski, M., et al. (2012). EARLY FLOWERING4 recruitment of EARLY FLOWERING3 in the nucleus sustains the Arabidopsis circadian clock. Plant Cell *24*, 428–43. Available at: http://www.pubmedcentral.nih.gov/articlerender.fcgi?artid=3315225&tool=pmcentrez&rendertype=abstract.

14. Helfer, A., Nusinow, D. A., Chow, B. Y., Gehrke, A. R., Bulyk, M. L., and Kay, S. A. (2011). LUX ARRHYTHMO encodes a nighttime repressor of circadian gene expression in the Arabidopsis core clock. Curr. Biol. *21*, 126–133.

15. Hicks, K. A., Albertson, T. M., and Wagner, D. R. (2001). EARLY FLOWERING3 encodes a novel protein that regulates circadian clock function and flowering in Arabidopsis. Plant Cell *13*, 1281–1292.

16. Mizuno, T., Nomoto, Y., Oka, H., Kitayama, M., Takeuchi, A., Tsubouchi, M., and Yamashino, T. (2014). Ambient Temperature Signal Feeds into the Circadian Clock Transcriptional Circuitry Through the EC Night-Time Repressor in Arabidopsis thaliana. Plant Cell Physiol. *0*, 1–19. Available at: http://www.ncbi.nlm.nih.gov/pubmed/24500967.

17. Kumar Lucyshyn, D., Jaeger, K.E., Alvey, E., Harberd, N. P., Wigge, P. A., V. (2012). The PIF4 Transcription factor mediates the thermal activation of flowering. Nature *in press*.

18. Nomoto, Y., Kubozono, S., Miyachi, M., Yamashino, T., Nakamichi, N., and Mizuno, T. (2012). A circadian clock-and PIF4-mediated double coincidence mechanism is implicated in the thermosensitive photoperiodic control of plant architectures in arabidopsis thaliana. Plant Cell Physiol. *53*, 1965–1973.

19. Steindler, C., Matteucci, A., Sessa, G., Weimar, T., Ohgishi, M., Aoyama, T., Morelli, G., and Ruberti, I. (1999). Shade avoidance responses are mediated by the ATHB-2 HD-zip protein, a negative regulator of gene expression. Development *126*, 4235–4245.

20. Anwer MU, Boikoglou E, Herrero E, Hallstein M, Davis AM, Velikkakam James G, Nagy F, D. S. (2014). Natural variation reveals that intracellular distribution of ELF3 protein is associated with function in the circadian clock. Elife *e02206*, 10.7554/eLife.02206.

21. Thines, B., and Harmon, F. G. (2010). Ambient temperature response establishes ELF3 as a required component of the core Arabidopsis circadian clock. Proc. Natl. Acad. Sci. U. S. A. *107*, 3257–3262.

22. Yu, J. W., Rubio, V., Lee, N. Y., Bai, S., Lee, S. Y., Kim, S. S., Liu, L., Zhang, Y., Irigoyen, M. L., Sullivan, J. A., et al. (2008). COP1 and ELF3 Control Circadian Function and Photoperiodic Flowering by Regulating GI Stability. Mol. Cell *32*, 617–630.

23. Dixon, L. E., Knox, K., Kozma-Bognar, L., Southern, M. M., Pokhilko, A., and Millar, A. J. (2011). Temporal repression of core circadian genes is mediated through EARLY FLOWERING 3 in Arabidopsis. Curr. Biol. *21*, 120–125.

24. Chow, B. Y., Helfer, A., Nusinow, D. A., and Kay, S. A. (2012). ELF3 recruitment to the PRR9 promoter requires other Evening Complex members in the Arabidopsis circadian clock. Plant Signal. Behav. *7*, 170–173.

25. Boden, S. a, Weiss, D., Ross, J. J., Davies, N. W., Trevaskis, B., Chandler, P. M., and Swain, S. M. (2014). EARLY FLOWERING3 Regulates Flowering in Spring Barley by Mediating Gibberellin Production and FLOWERING LOCUS T Expression. Plant Cell. Available at: http://www.ncbi.nlm.nih.gov/pubmed/24781117.

26. Faure, S., Turner, A. S., Gruszka, D., Christodoulou, V., Davis, S. J., von Korff, M., and Laurie, D. A. (2012). Mutation at the circadian clock gene EARLY MATURITY 8 adapts domesticated barley (Hordeum vulgare) to short growing seasons. Proc. Natl. Acad. Sci. *109*, 8328–8333.

Supplemental Information:

Supplemental information includes materials and methods, 4 additional figures and 4 additional tables.

Acknowledgments:

The authors wish to thank Yaroslav Lazarev (Stemmer Imaging Ltd, UK) for developing a custom time-lapse imaging application and George Artavanis for help in differentiating growth rates. We thank Steve Kay for providing seeds. This work was made possible by the award of a European Research Council Starting Grant to PW (EC FP7 ERC 243140). The work in PW's laboratory is supported by a Fellowship from the Gatsby Foundation (GAT3273/GLB).

Author contributions:

PW and MB conceived the study. PW, AK and AG phenotyped the MAGIC lines. BH and MB performed QTL mapping, association analysis and identified candidate genes with help from DJ. MB and ES performed phenotypic characterisation, complementation and gene expression analyses. MB, AW and TH performed circadian analyses. MD and JL performed mathematical modeling and numerical simulations. SY generated the ELF3 tagged line. KJ performed ChIP. PW, MB, BH, JL and MD wrote the manuscript. All authors discussed and commented on the manuscript.

Figure Legends

Figure 1. Warm temperature results in greater night-time growth and there is considerable natural variation in this trait. (A) Hypocotyl lengths of Col-0 at the end of an infrared (IR) imaging period at 22 and 27 ºC, see 1B. Data plotted are mean ± SD, n=40. (B) Differentiated growth rate of Col-0 at 22 and 27 ºC derived from IR imaging (inset: image of 5-day old Col-0 seedlings grown in SD at 22 and 27 ºC after 48h germination at 22 ºC. Image taken at the end of the IR time course in 1B. Data plotted are mean ± SD, n=8. (C) Natural variation in hypocotyl length in MAGIC parental lines at 12, 22 and 27 ºC. Data plotted are mean ± SD, n=40. (D) Density plot of hypocotyl

length in MAGIC lines at 12, 22 and 27 ºC showing transgressive segregation. Coloured triangles indicate the phenotypic range of hypocotyl length in MAGIC parents. (E) Interval Mapping QTL plot with permutation derived genome wide significance line. Names of QTL correspond to those in Table S2.

Figure 2. Natural variation in *ELF3* and *LUX* changes thermosensory growth and *elf3-1* has a constitutive warm temperature response. (A) Founder effect estimates of selected parents for major QTL on Chr2 and 3 at 22 ºC corresponding to parents tested in complementation analysis, see Figure 2C. Allele effect estimates for all MAGIC parents are shown in Figure S2. (B) RAE and period estimates derived from Delayed Fluorescence (DF) data obtained from BRASS for most of the MAGIC parents. Note Sf-2, predicted to have a weak ELF3 allele, has the least rhythmic clock. See Figure S2 for DF traces. Blue dots are the mean, grey dots are the individual measurements. RAE and period estimates were 0.52, 25.9 h for *elf3-1* (n=3 rhythmic samples) and 0.65, 20.9 h for *lux-4* (n=4 rhythmic samples). (C) Quantitative complementation cross (QCC) analysis for selected MAGIC line parents predicted to contribute most to Chr 2 and 3 QTL at 22 ºC. Compare the pattern of gold dots in the accession x mutant F1 to the predictions in Figure 2A. Matching pattern confirms *PHYB*, *ELF3* and *LUX* are quantitative trait genes for QTL. Data plotted are mean ± SD, n=40 from at least two independent crosses. (D) Growth of MAGIC parents with weak alleles of *ELF3* and *LUX* at 22 ºC. Accessions specifically exhibit more growth at night consistent with weak *ELF3* and/or *LUX* (final length and growth rate at 22 and 27 ºC in Figure S2). (E) Growth of *elf3-1* 22 and 27 ºC (final length in Figure S2). (F) Growth of *lux-4* 22 and 27 ºC (final length in Figure S2). Data plotted in D-F are mean ± SD, n=8.

Figure 3. The thermoresponsiveness of *PIF4* expression is mediated by *ELF3*. (A) Expression of *PIF4* at 22 ºC (orange) and 27 ºC (red). (B) Expression of *ATHB2* at 22 ºC and 27 ºC. (C) Expression of *ELF3* at 22 ºC and 27 ºC. (D) Expression of *LUX* at 22 ºC and 27 ºC. (E) Expression of *ELF4* at 22 ºC and 27 ºC. See Figure S4 for further

characterization of Ws-0 and Zu-0. Data plotted are mean ± SE, n=3 independent biological experiments.

Figure 4. ELF3 rapidly and reversibly communicates temperature status information directly to the promoters of responsive genes. (A) Modeling results for *PIF4* expression at 22 ºC and 27 ºC (orange and red lines) compared with experimental results (black circles; Figure 3A) in different backgrounds. For Col-0, a simple temperature-dependent repressor (R) model captures *PIF4* thermoresponsiveness. The temperature-dependent repressor is unlikely to be the EC, since setting R = 0 does not accurately capture the behavior of *PIF4* in the *lux-4* background (black dashed line: R = 0). By contrast, allowing a certain level of R activity to be retained enables the model to fit the expression data well (orange and red lines for *lux-4* and *elf3-1*). (B) Repressor (R) was quantified for the night periods in the different backgrounds and scaled for median expression of *PIF4* at 27°C. Both Col-0 and *lux-4* retain thermal responsiveness, while *elf3-1* does not. (C) Expression of *LUX* in Col-0 or *elf3-1* for plants grown at constant 22 ºC (orange), constant 27 ºC (red) or shifted to a different temperature at the end of the day (8 h) prior to sampling during the subsequent night (22 to 27 ºC, orange dotted; 27 to 22 ºC, red dotted). Data plotted are mean ± SE, n=3 independent biological experiments. (D) Binding of ELF3 or ELF4 at target promoters by Chromatin Immunopurification (ChIP). Binding at the promoters of *LUX*, *PIF4* and *PRR9* in seedlings at a constant 22 ºC or for plants shifted to 27 ºC at the end of the day (as in C) and sampled after 2 hours of darkness. Amplicons in the *LUX* coding region were used as a negative control. Identical ChIP experiments were also performed on the untagged background (Col-0). See Figure S4 for further characterization of ChIP lines. Data plotted are mean ± SE, n=3 independent biological experiments, each assayed in triplicate.

Figure

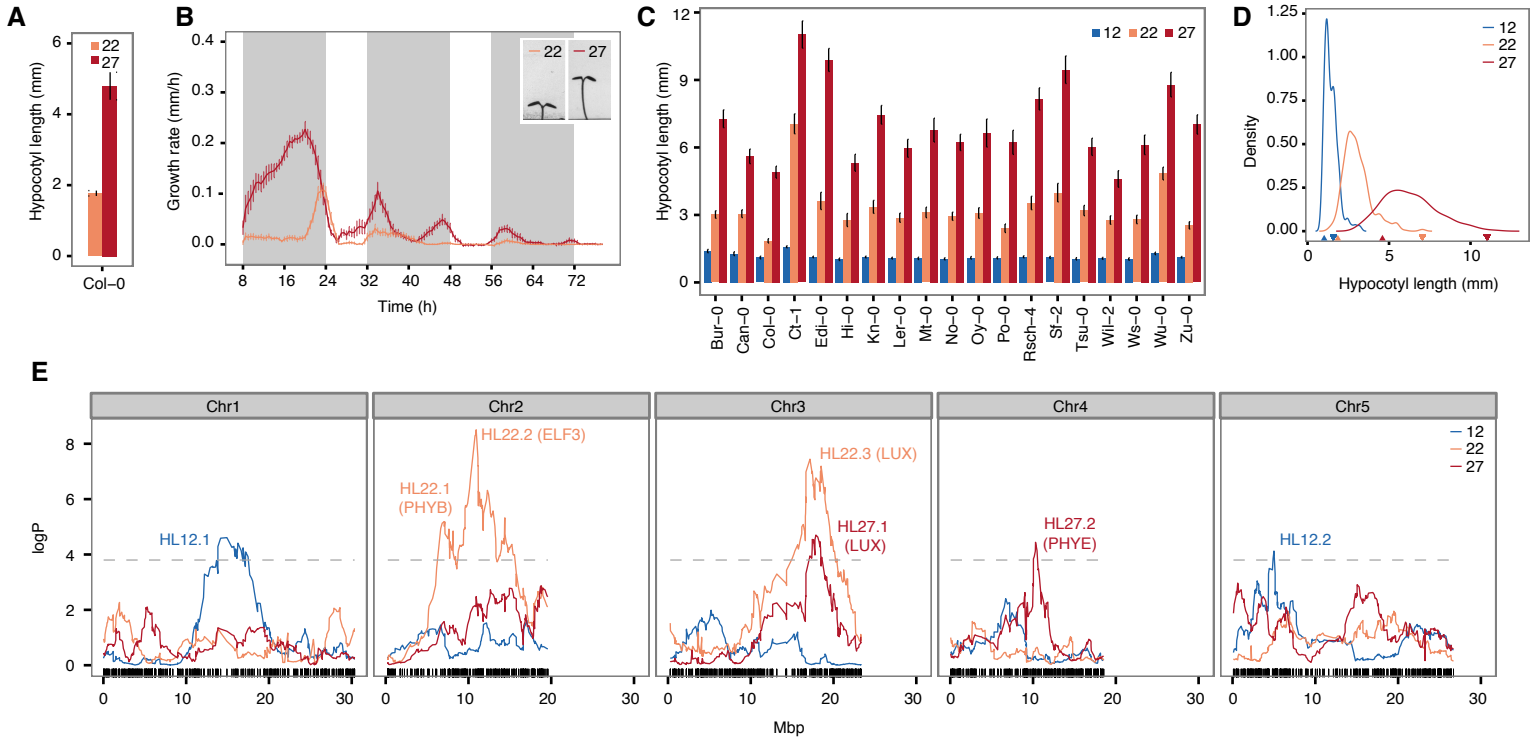
A
Hypocotyl length (mm)
22
27
Col–0
B
Growth rate (mm/h)
Time (h)
C
Hypocotyl length (mm)
12 22 27
Bur–0
Can–0
Col–0
Ct–1
Edi–0
Hi–0
Kn–0
Ler–0
Mt–0
No–0
Oy–0
Po–0
Rsch–4
Sf–2
Tsu–0
Wil–2
Ws–0
Wu–0
Zu–0
D
Density
Hypocotyl length (mm)

E
Chr1
Chr2
Chr3
Chr4
Chr5
logP
HL12.1
HL22.2 (ELF3)
HL22.1 (PHYB)
HL22.3 (LUX)
HL27.1 (LUX)
HL27.2 (PHYE)
HL12.2
Mbp

Figure

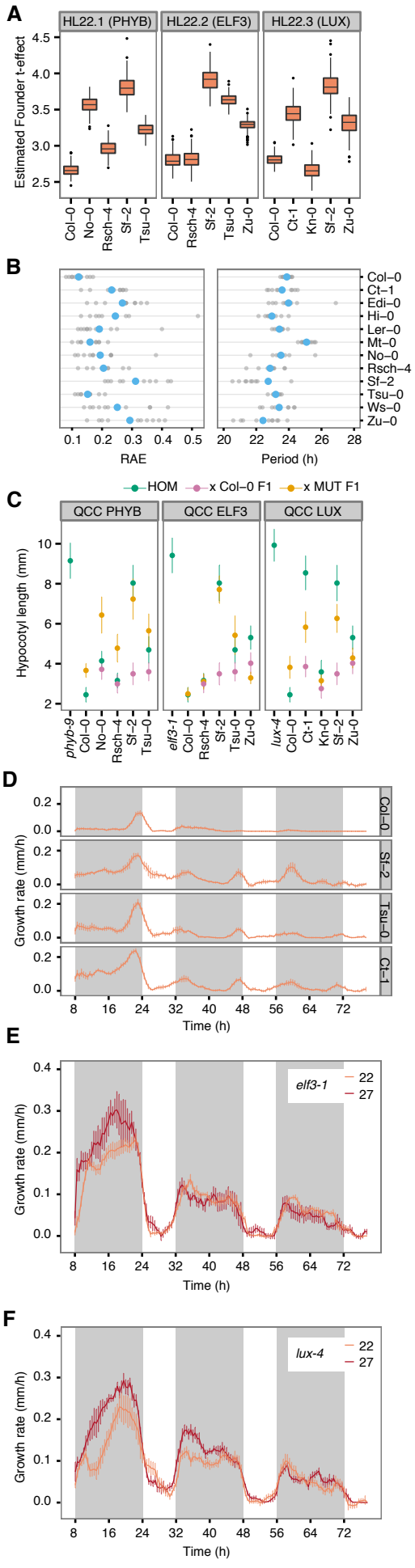
A
HL22.1 (PHYB)
HL22.2 (ELF3)
HL22.3 (LUX)
Estimated Founder t-effect
B
RAE
Period (h)
C
HOM
x Col–0 F1
x MUT F1
QCC PHYB
QCC ELF3
QCC LUX
Hypocotyl length (mm)
D
Growth rate (mm/h)
Time (h)
E
elf3-1
22
27
F
lux-4

Figure

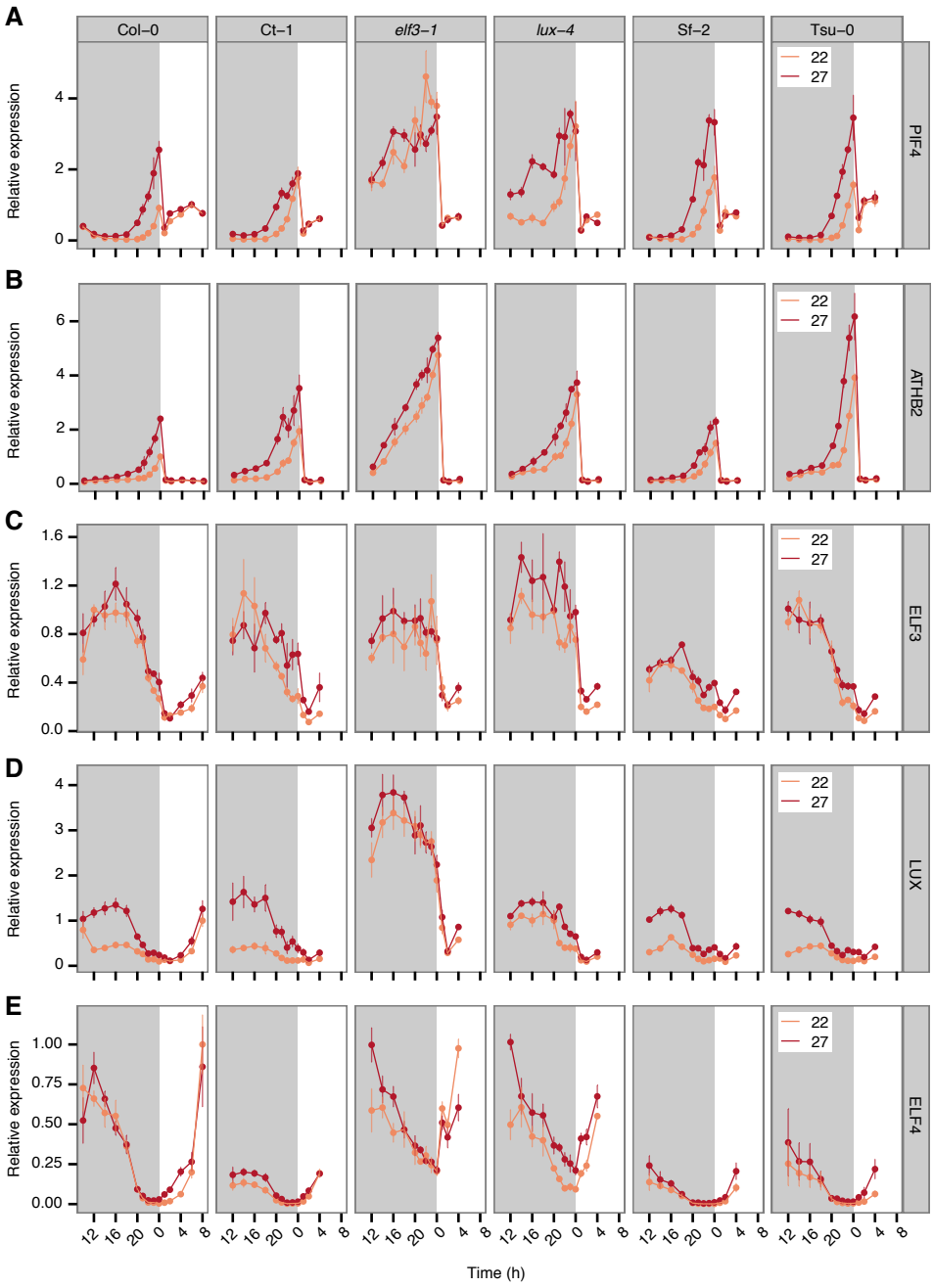
A
B
C
D
E
Col−0
Ct−1
elf3−1
lux−4
Sf−2
Tsu−0
22
27
PIF4
ATHB2
ELF3
LUX
ELF4
Relative expression
Time (h)

Figure

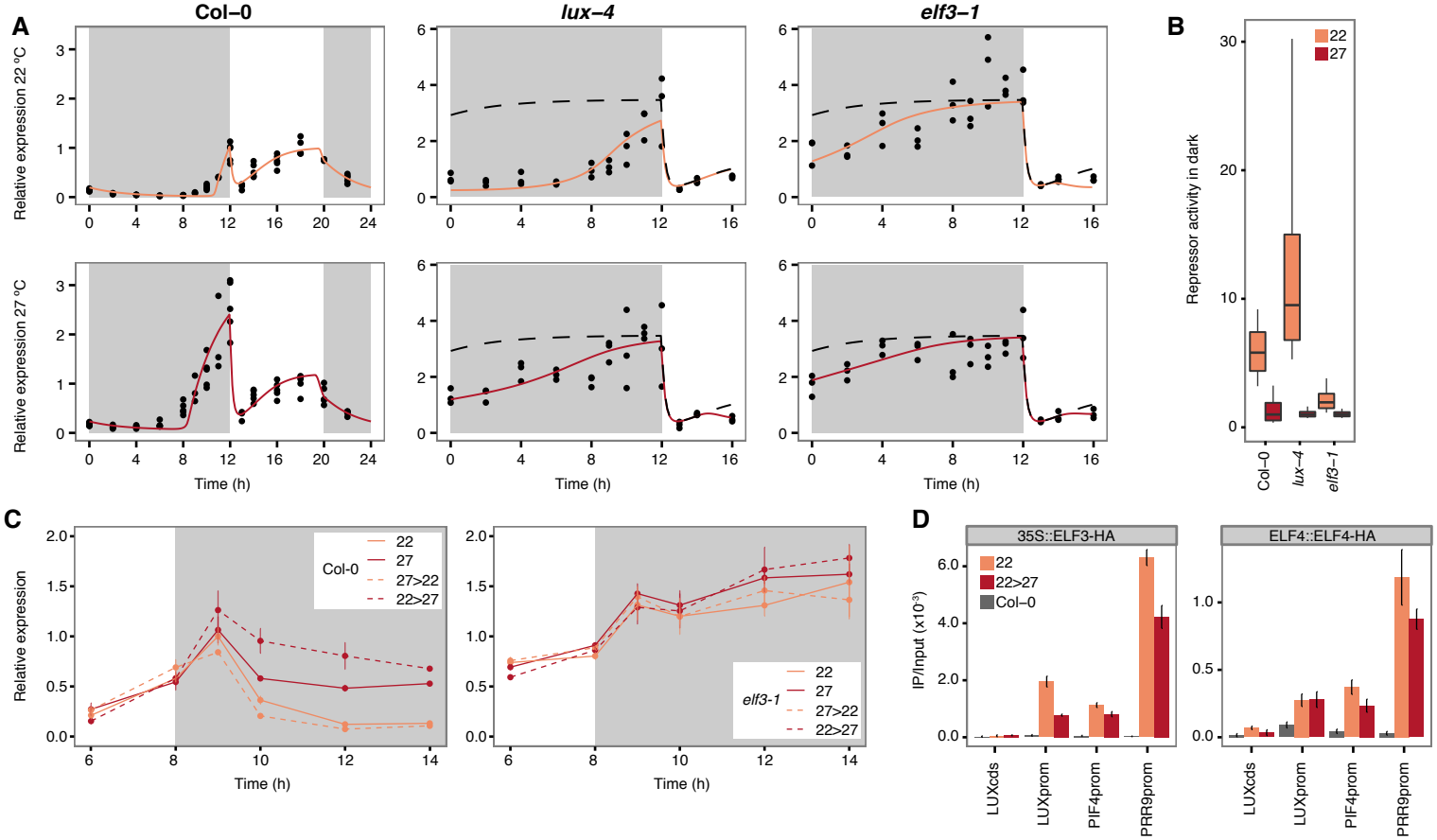
A
Col–0
lux–4
elf3–1
Relative expression 22 °C
Relative expression 27 °C
Time (h)
B
Repressor activity in dark
22
27
Col–0
lux–4
elf3–1
C
Relative expression
Col-0
22
27
27>22
22>27
elf3-1
Time (h)
D
35S::ELF3-HA
ELF4::ELF4-HA
IP/Input (x10⁻³)
22
22>27
Col–0
LUXcds
LUXprom
PIF4prom
PRR9prom

Supplementary Information

Supplementary Figures

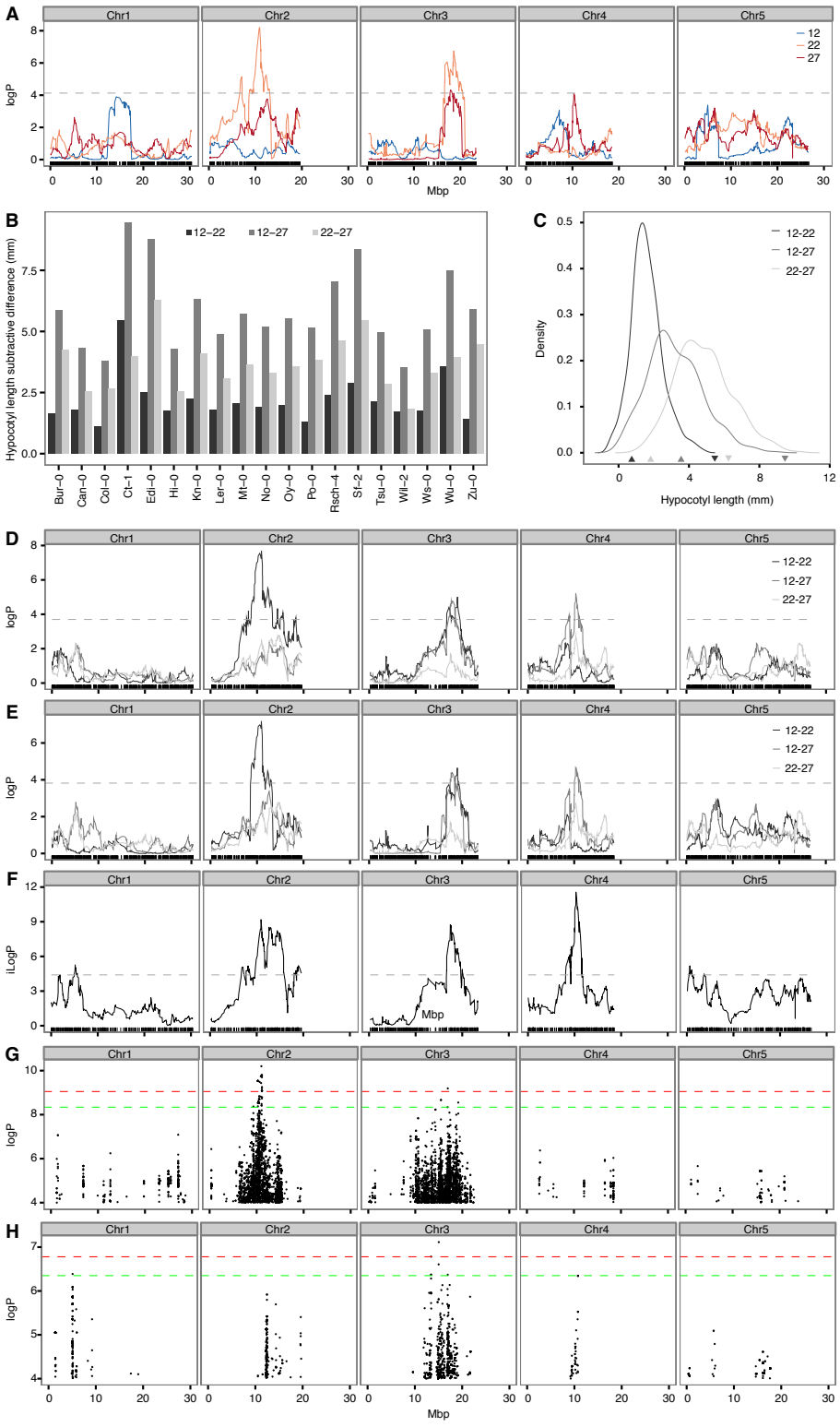
A
Chr1
Chr2
Chr3
Chr4
Chr5
12
22
27
logP
Mbp
B
12–22
12–27
22–27
Hypocotyl length subtractive difference (mm)
Bur–0
Can–0
Col–0
Ct–1
Edi–0
Hi–0
Kn–0
Ler–0
Mt–0
No–0
Oy–0
Po–0
Rsch–4
Sf–2
Tsu–0
Wil–2
Ws–0
Wu–0
Zu–0
C
12-22
12-27
22-27
Density
Hypocotyl length (mm)
D
E
F
iLogP
G
H

Figure S1, related to Figure 1. (A) Composite Interval Mapping at 12, 22 and 27 ºC. (B) Natural variation in thermal responsiveness in MAGIC parents calculated by pairwise subtractive difference. (C) Density plot of hypocotyl length difference in MAGIC lines at 12, 22 and 27 ºC showing transgressive segregation. Triangles indicate phenotypic range of hypocotyl length in MAGIC parents. (D) Interval Mapping hypocotyl length subtractive differences in MAGIC lines. (E) Composite Interval Mapping hypocotyl length subtractive differences in MAGIC lines. (F) Multivariate interval mapping modeling hypocotyl length at all three temperatures simultaneously. In A and D-F dashed lines indicate the permutation derived genome wide significance threshold. Association analysis performed on hypocotyl traits in MAGIC lines using 'genome_scan' with 3 million varying sites at 22 ºC (G) and 27 ºC (H). Dashed lines indicate the permutation derived genome wide significance threshold (red 0.05; green 0.10 genomewide significance).

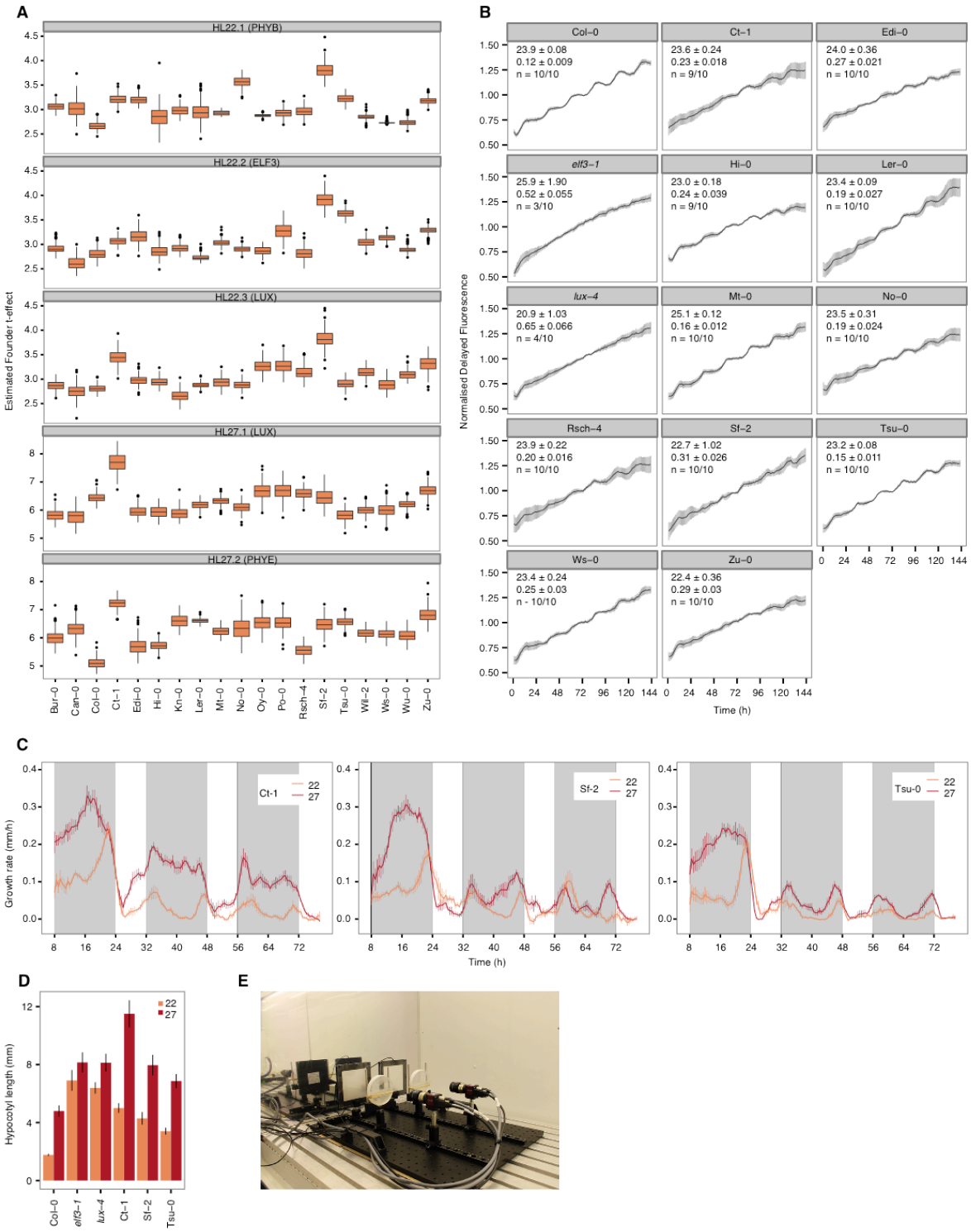
A
HL22.1 (PHYB)
HL22.2 (ELF3)
HL22.3 (LUX)
HL27.1 (LUX)
HL27.2 (PHYE)
Estimated Founder t-effect
Bur–0 Can–0 Col–0 Ct–1 Edi–0 Hi–0 Kn–0 Ler–0 Mt–0 No–0 Oy–0 Po–0 Rsch–4 Sf–2 Tsu–0 Wil–2 Ws–0 Wu–0 Zu–0
B
Col–0
Ct–1
Edi–0
elf3–1
Hi–0
Ler–0
lux–4
Mt–0
No–0
Rsch–4
Sf–2
Tsu–0
Ws–0
Zu–0
Normalised Delayed Fluorescence
Time (h)
C
Ct-1
Sf-2
Tsu-0
22
27
Growth rate (mm/h)
Time (h)
D
Hypocotyl length (mm)
Col–0 elf3–1 lux–4 Ct–1 Sf–2 Tsu–0
E

19

20

Figure S2, related to Figure 2. (A) Allele effect estimates for all MAGIC parents for which significant hypocotyl length QTL were detected at 22 ºC and 27 ºC. (B) Delayed Fluorescence (DF) traces for selected MAGIC parents. Output from BRASS software including period (top), RAE (middle) and number of rhythmic samples (bottom) are indicated in each panel as mean ± SE. DF trace data plotted are mean ± SD. (C) Ct-1, Sf-2 and Tsu-0 growth dynamics at 22 (orange) and 27 ºC (red). (D) Final hypocotyl length for Col-0, selected MAGIC parents and *elf3-1*, *lux-4* in IR growth dynamics experiments. Data plotted are mean ± SD, n=8 in A-C and n=40 in D. (E) Custom IR imaging rig developed for this study.

```
Col-0           MKRGKDEEKILEPMFPRLHVNDADKGGPRAPPRNKMALYEQLSIPSQRFGDHGTMNSRSN
Ct-1            MKRGKDEEKILEPMFPRLHVNDADKGGPRAPPRNKMALYEQLSIPSQRFGDHGTMNSRSN
Sf-2            MKRGKDEEKILEPMFPRLHVNDADKGGPRAPPRNKMALYEQLSIPSQRFGDHGTMNSRSN
Tsu-0           MKRGKDEEKILEPMFPRLHVNDADKGGPRAPPRNKMALYEQLSIPSQRFGDHGTMNSRSN
Rsch-4          MKRGKDEEKILEPMFPRLHVNDADKGGPRAPPRNKMALYEQLSIPSQRFGDHGTMNSRSN
Zu-0            MKRGKDEEKILEPMFPRLHVNDADKGGPRAPPRNKMALYEQLSIPSQRFGDHGTMNSRSN
                ************************************************************

Col-0           NTSTLVHPGPSSQPCGVERNLSVQHLDSSAANQATEKFVSQMSFMENVRSSAQHDQRKMV
Ct-1            NTSTLVHPGPSSQPCGVERNLSVQHLDSSAANQATEKFVSQMSFMENVRSSAQHDQRKMV
Sf-2            NTSTLVHPGPSSQPCGVERNLSVQHLDSSAANQATEKFVSQMSFMENVRSSAQHDQRKMV
Tsu-0           NTSTLVHPGPSSQPCGVERNLSVQHLDSSAANQATEKFVSQMSFMENVRSSAQHDQRKMV
Rsch-4          NTSTLVHPGPSSQPCGVERNLSVQHLDSSAANQATEKFVSQMSFMENVRSSAQHDQRKMV
Zu-0            NTSTLVHPGPSSQPCGVERNLSVQHLDSSAANQATEKFVSQMSFMENVRSSAQHDQRKMV
                ************************************************************

Col-0           REEEDFAVPVYINSRRSQSHGRTKSGIEKEKHTPMVAPSSHHSIRFQEVNQTGSKQNVCL
Ct-1            REEEDFAVPVYINSRRSQSHGRTKSGIEKEKHTPMVAPSSHHSIRFQEVNQTGSKQNVCL
Sf-2            REEEDFAVPVYINSRRSQSHGRTKSGIEKEKHTPMVAPSSHHSIRFQEVNQTGSKQNVCL
Tsu-0           REEEDFAVPVYINSRRSQSHGRTKSGIEKEKHTPMVAPSSHHSIRFQEVNQTGSKQNVCL
Rsch-4          REEEDFAVPVYINSRRSQSHGRTKSGIEKEKHTPMVAPSSHHSIRFQEVNQTGSKQNVCL
Zu-0            REEEDFAVPVYINSRRSQSHGRTKSGIEKEKHTPMVAPSSHHSIRFQEVNQTGSKQNVCL
                ************************************************************

Col-0           ATCSKPEVRDQVKANARSGGFVISLDVSVTEEIDLEKSASSHDRVNDYNASLRQESRNRL
Ct-1            ATCSKPEVRDQVKANARSGGFVISLDVSVTEEIDLEKSASSHDRVNDYNASLRQESRNRL
Sf-2            ATCSKPEVRDQVKANARSGGFVISLDVSVTEEIDLEKSASSHDRVNDYNASLRQESRNRL
Tsu-0           ATCSKPEVRDQVKANARSGGFVISLDVSVTEEIDLEKSASSHDRVNDYNASLRQESRNRL
Rsch-4          ATCSKPEVRDQVKANARSGGFVISLDVSVTEEIDLEKSASSHDRVNDYNASLRQESRNRL
Zu-0            ATCSKPEVRDQIKANARSGGFVISLDVSVTEEIDLEKSASSHDRVNDYNASLRQESRNRL
                ***********:************************************************

Col-0           YRDGGKTRLKDTDNGAESHLATENHSQEGHGSPEDIDNDREYSKSRACASLQQINEEASD
Ct-1            YRDGGKTRLKDTDNGAESHLATENHSQEGHGSPEDIDNDREYSKSRACASLQQINEEASD
Sf-2            YRDGGKTRLKDTDNGAESHLATENHSQEGHGSPEDIDNDREYSKSRACASLQQINEEASD
Tsu-0           YRDGGKTRLKDTDNGAESHLATENHSQEGHGSPEDIDNDREYSKSRACASLQQINEEASD
Rsch-4          YRDGGKTRLKDTDNGAESHLATENHSQEGHGSPEDIDNDREYSKSRACASLQQINEEASD
Zu-0            YRDGGKTRLKDTDNGAESHLATENHSQEGHGSPEDIDNDREYSKSRACASLQQINEEASD
                ************************************************************

Col-0           DVSDDSMVDSISSIDVSPDDVVGILGQKRFWRARKAIANQQRVFAVQLFELHRLIKVQKL
Ct-1            DVSDDSMVDSISSIDVSPDDVVGILGQKRFWRARKAIANQQRVFAVQLFELHRLIKVQKL
Sf-2            DVSDDSMVDSISSIDVSPDDVVGILGQKRFWRARKAIANQQRVFAVQLFELHRLIKVQKL
Tsu-0           DVSDDSMVDSISSIDVSPDDVVGILGQKRFWRARKAIANQQRVFAVQLFELHRLIKVQKL
Rsch-4          DVSDDSMVDSISSIDVSPDDVVGILGQKRFWRARKAIANQQRVFAVQLFELHRLIKVQKL
Zu-0            DVSDDSMVDSISSIDVSPDDVVGILGQKRFWRARKAIANQQRVFAVQLFELHRLIKVQKL
                ************************************************************

Col-0           IAASPDLLLDEISFLGKVSAKSYPVKKLLPSEFLVKPPLPHVVVKQRGDSEKTDQHKMES
Ct-1            IAASPDLLLDEISFLGKVSAKSYPVKKLLPSEFLVKPPLPHVVVKQRGDSEKTDQHKMES
Sf-2            IAASPDLLLDEISFLGKVSAKSYPVKKLLPSEFLVKPPLPHVVVKQRGDSEKTDQHKMES
Tsu-0           IAASPDLLLDEISFLGKVSAKSYPVKKLLPSEFLVKPPLPHVVVKQRGDSEKTDQHKMES
Rsch-4          IAASPDLLLDEISFLGKVSAKSYPVKKLLPSEFLVKPPLPHVVVKQRGDSEKTDQHKMES
Zu-0            IAASPDLLLDEISFLGKVSAKSYPVKKLLPSEFLVKPPLPHVVVKQRGDSEKTDQHKMES
                ************************************************************

Col-0           SAENVVGRLSNQGHHQQSNYMPFANNPPASPAPNGYCFPPQPPPSGNHQQWLIPVMSPSE
Ct-1            SAENVVGRLSNQGHHQQSNYMPFANNPPASPAPNGYCFPPQPPPSGNHQQWLIPVMSPSE
Sf-2            SAENVVGRLSNQGHHQQSNYMPFANNPPASPAPNGYCFPPQPPPSGNHQQWLIPVMSPSE
Tsu-0           SAENVVGRLSNQGHHQQSNYMPFANNPPASPAPNGYCFPPQPPPSGNHQQWLIPVMSPSE
Rsch-4          SAENVVGRLSNQGHHQQSNYMPFANNPPASPAPNGYCFPPQPPPSGNHQQWLIPVMSPSE
Zu-0            SAENVVGRLSNQGHHQQSNYMPFANNPPASPAPNGYCFPPQPPPSGNHQQWLIPVMSPSE
                ************************************************************

Col-0           GLIYKPHPGMAHTGHYGGYYGHYMPTPMVMPQYHPGMGFPPPGNGYFPPYGMMPTIMNPY
Ct-1            GLIYKPHPGMAHTGHYGGYYGHYMPTPMVMPQYHPGMGFPPPGNGYFPPYGMMPTIMNPY
Sf-2            GLIYKPHPGMAHTGHYGGYYGHYMPTPMVMPQYHPGMGFPPPGNGYFPPYGMMPTIMNPY
Tsu-0           GLIYKPHPGMAHTGHYGGYYGHYMPTPMVMPQYHPGMGFPPPGNGYFPPYGMMPTIMNPY
Rsch-4          GLIYKPHPGMAHTGHYGGYYGHYMPTPMVMPQYHPGMGFPPPGNGYFPPYGMMPTIMNPY
Zu-0            GLIYKPHPGMAHTGHYGGYYGHYMPTPMVMPQYHPGMGFPPPGNGYFPPYGMMPTIMNPY
                ************************************************************

Col-0           CSS-----QQQQQQQPNEQMNQFGHPGNLQNTQQQQQRSDNEPAPQQQQQPTKSYPRARK
Ct-1            CSS-----QQQQQQQPNEQMNQFGHPGNLQNTQQQQQRSDNEPAPQQQQQPTKSYPRARK
Sf-2            CSS-----QQQQQQQPNEQMNQFGHPGNLQNTQQQQQRSDNEPAPQQQQQPTKSYPRARK
Tsu-0           CSS-----QQQQQQQPNEQMNQFGHPGNLQNTQQQQQRSDNEPAPQQQQQPTKSYLRARK
Rsch-4          CSS-QQQQQQQQQQQPNEQMNQFGHPGNLQNTQQQQQRSDNEPAPQQQQQPTKSYPRARK
```

```
Zu-0            CSSQQQQQQQQQQQQPNEQMNQFGHPGNLQNTQQQQQRSDNEPAPQQQQQPTKSYPRARK
                ***     ********************************************** ****

Col-0           SRQGSTGSSPSGPQGISGSKSFRPFAAVDEDSNINNAPEQTMTTTTTTTRTTVTQTTRDG
Ct-1            SRQGSTGSSPSGPQGISGSKSFRPFAAVDEDSNINNAPEQTMTTTTTTTRTTVTQTTRDG
Sf-2            SRQGSTGSSPSGPQGISGSKSFRPFAAVDEDSNINNAPEQTMTTTTTTTRTTVTQTTRDG
Tsu-0           SRQGSTGSSPSGPQGISGSKSFRPFAAVDEDSNINNAPEQTMTTTTTTTRTTVTQTTRDG
Rsch-4          SRQGSTGSSPSGPQGISGSKSFRPFAAVDEDSNINNAPEQTMTTTTTTTRTTVTQTTRDG
Zu-0            SRQGSTGSSPSGPQGISGSKSFRPFAAVDEDSNINNAPEQTMTTTTTTTRTTVTQTTRDG
                ************************************************************

Col-0           GGVTRVIKVVPHNAKLASENAARIFQSIQEERKRYDSSKP
Ct-1            GGVTRVIKVVPHNAKLASENAARIFQSIQEERKRYDSSKP
Sf-2            GGVTRVIKVVPHNAKLASENAARIFQSIQEERKRYDSSKP
Tsu-0           GGVTRVIKVVPHNAKLASENAARIFQSIQEERKRYDSSKP
Rsch-4          GGVTRVIKVVPHNAKLASENAARIFQSIQEERKRYDSSKP
Zu-0            GGVTRVIKVVPHNAKLASENAARIFQSIQEERKRYDSSKP
                ****************************************
```

Figure S3, related to Figure 3. ClustalW alignment of ELF3 protein in selected MAGIC parents. Alignment performed using default parameters. Amino acid sequences were obtained from http://mus.well.ox.ac.uk/19genomes/magic.html

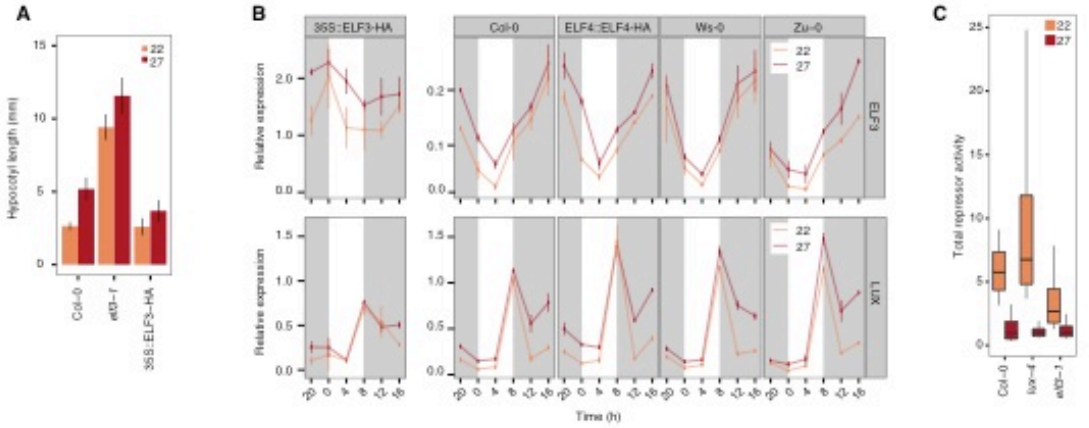
A
Hypocotyl length (mm)
22
27
Col-0
elf3-1
35S::ELF3-HA
B
35S::ELF3-HA
Col-0
ELF4::ELF4-HA
Ws-0
Zu-0
Relative expression
ELF3
LUX
Time (h)
C
Total repressor activity
lux-4

Figure S4, related to Figure 4. (A) Hypocotyl length measurements at 22 and 27 ºC under SD for 35S::ELF3-HA. Data plotted are mean ± SD, n=40. (B) Expression of *ELF3* and *LUX* in 35S::ELF3-HA (this study), ELF4::ELF4-HA [1], Ws-0 and Zu-0. Data plotted are mean ± SD, n=2 independent biological experiments. (C) Repressor activity over the full 24h period scaled by the median level at 27 ºC in the relevant background.

Supplementary Tables

Trait	Min	Max	n_P	n_L	h_P^2	h_L^2
Avg.12	0.73	3.4	4944	412	0.983	0.9985
Avg.22	1.2	7.2	5112	426	0.992	0.9993
Avg.27	3.0	11.9	4908	409	0.997	0.9998

Factor	Z	P
Genotype	5.91	<0.001
Temperature	1.00	0.32
Genotype x Temperature	20.2	<0.001

Table S1. Range and heritability for the traits measured. h_P^2 is the heritability of individual plants, h_L^2 represents the heritability of the phenotype averaged across replicates within MAGIC lines. n_p denotes number of plants, while n_L is the number of MAGIC lines assayed in each condition. We decompose the variance by fitting additional random effects for temperature and genotype-temperature interaction. The significance of each factor's contribution to the variance is assessed by the magnitude of the Z-statistic for the variance estimate, computed by dividing the estimate of the variance by its standard error.